RESEARCH PAPER

Properties of CdS Thin Films Prepared by Thermal Evaporation

Eman M. Noori

Radiology department, Institute of Medical Technology- Baghdad, Middle Technical University, Iraq

ARTICLE INFO

Article History:
Received 08 October 2023
Accepted 17 December 2023
Published 01 January 2024

Keywords:
Band gap
Thermal evaporation
Thin cadmium sulfide films
Transmission
X-ray diffraction (XRD)

ABSTRACT

Thermal evaporation was used to create pure CdS thin films, which were then analyzed using XRD and UV-VIS spectroscopy. With changes in thickness, it was discovered that the particle size decreased from 23.6 nm to 21.7 nm. From the XRD data, the impact of thickness on strain and dislocation has been estimated. To determine how optical characteristics changed as thickness changed, transmission data were examined in the 200–1100 nm spectral range. Additionally, it was found that as thickness increased, between 2.444 and 2.401 eV, the band gap decreased.

How to cite this article
Noori E. M. Pluronic based nano-delivery systems; Prospective warrior in war against cancer. J Nanostruct, 2024; 14(1):12-19.
DOI: 10.22052/JNS.2024.01.002

INTRODUCTION

Research on group II–VI chalcogenide semiconductors has attracted a lot of attention because it can be used to create nanostructured thin films that can be used to create cutting-edge optoelectronic devices. One of the most important components of this family is thought to be CdS [1], because it has transparency characteristics in the visible zone [2], a widespread 2.4 eV for the direct bandgap at room temperature [3-5], and a refractive index of 2.5 [6]. Studies on its structural and optical properties have thankfully been successful in the past few years in order to assess its technological potential for producing inexpensive and energy-efficient devices, such as photoconductive sensors [7], light-emitting diodes [8], logic circuits [1], solar cells [2], and so on. To fabricate CdS thin films, numerous techniques have been used, such as chemical bath deposition (CBD) [9], spray pyrolysis technique [10], electron beam vacuum evaporation [11], thermal evaporation [12], molecular beam epitaxy [13], liquid-phase deposition [14], pulsed laser deposition [15], and close space vapor transport (CSVT) [16].

Because it is a hassle-free and controlled method, the thermal evaporation approach has been used in this study to produce CdS thin films. The focus of the current investigation is on how the thickness of thermal evaporation-grown CdS polycrystalline thin films affects their structural and optical characteristics. The samples are characterized using X-ray diffraction (XRD) and the UV-VIS model of a spectrophotometer. The optical spectra are used to estimate optical constants such as the optical band gap, extinction coefficient, and refractive index.

MATERIALS AND METHODS

Because it is simple, thermal evaporation is needed to produce thin films of CdS, and the method also produces adhesion layers that are equally thin but smooth, controlled, and uniform.

* *Corresponding Author Email: dr.emanm.noori@mtu.edu.iq*

(CdS) powder with a high purity (99.99%) was used in order to make CdS thin films and placed in a molybdenum crucible as the evaporation source. The substrate and crucible were separated by 15 cm. The glass slides (substrates) were washed for ten to fifteen minutes in an ultrasonic bath containing acetone and distilled water, respectively, and then dried in the air. The evaporation was done at a high vacuum. The chamber pressure was kept at 1 mbar throughout the whole deposition operation. films prepared at room temperature with different thicknesses of 200 nm, 300 nm, 400 nm, and 500 nm. Cu Kα energy with a wavelength of 0.154 nm was employed in X-ray diffraction to explain the crystal structure characteristics of different films. The range of XRD was recorded at 2θ = 10°–70°. The UV-Vis spectrophotometer was used to record the transmittance spectra for prepared samples between 400 and 1100 nm.

RESULTS AND DISCUSSION

X-ray diffraction (XRD): At various thicknesses, CdS thin films' crystal structure and crystalline type are identified and confirmed using this non-destructive mechanism. The diffraction angle's measuring range was 2θ=10° to 70°. As far as we are aware, the structure of bulk CdS is either cubic or hexagonal [13]. Thin CdS films of various thicknesses are shown in Fig. 1 as diffraction patterns. Due to the diffraction planes (002), (100), (101), and (103), analysis of XRD emphasized the formation of a pure hexagonal structure (ICSD card 043599) and explained polycrystalline behavior. All of the films' highest intensity peaks, (002) correspond to the preferred orientation. The clusters in the films exhibit a columnar structure in the direction perpendicular to the film surface as a result of this outcome [17].

The Scherrer equation was used to get the grain

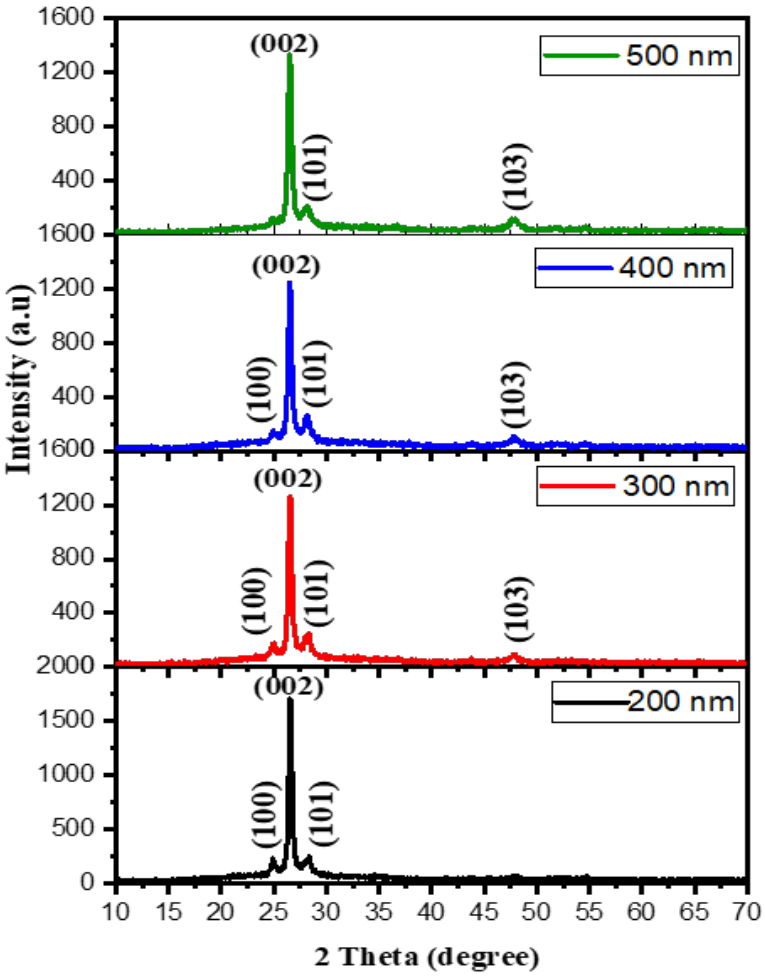

Fig. 1. CdS films' X-ray diffraction spectra at various thicknesses.

size (D) using the formula below [18]:

$$D = 0.9\lambda/\beta COS\theta \quad (1)$$

Here, θ is the diffraction peak angle in radians, β is the full-width at half-maximum of the peak with the highest intensity, and λ is the wavelength of the source employed. Fig. 2 depicts how the grain size varies with thickness. This graphic shows clearly that the grain size increased at a thickness of 200 nm and subsequently reduced as the thickness increased. The degree of structure defects increases as grain boundaries increase and grain size decreases[5].

The length of the dislocation lines in relation to volume is used to indicate the dislocation density, which has been calculated using equation [2] (see[16]).

$$\delta = 1/D^2 \quad (2)$$

where (δ) is a measure of the degree of crystal imperfection. Therefore, the tiny values of (δ) found in the current investigation supported the CdS films' excellent crystallinity. Table 1 provides the values.

The following formula was used to calculate the films' strain (ε) [19].

$$\varepsilon = \beta\cos\theta/4 \quad (3)$$

Fig. 2 represents the relationship between the strain and thickness of thin CdS films. It is clear that as thickness increases, strain first reduces and then increases; this change in strain shows that as thickness rises, the concentration of lattice defects also rises. In order to obtain comprehensive information on the structural features, Table 1 summarizes the computed grain size values (D), dislocation density (δ) and strain (ε) along the

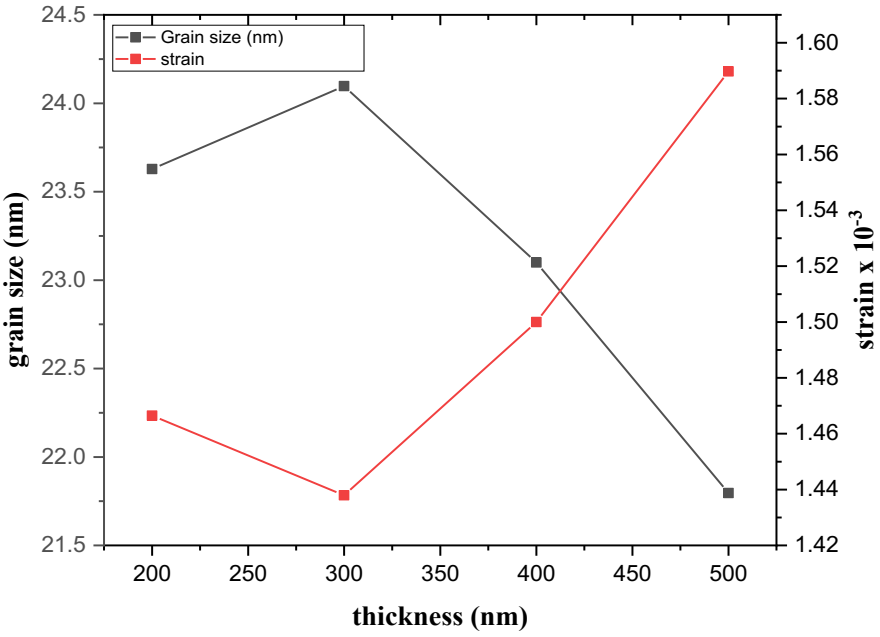

Fig. 2. shows how stress and grain size vary with thickness.

Table 1. The structural characteristics of CdS thin films that were formed at various thicknesses were determined from 002 peaks.

thicknesses (nm)	2θ(deg)	D (nm)	δ (x 10^{15}) lines/ $(m)^2$	ε x 10^{-3}
200	26.56651	23.62811	1.7911923	1.466474
300	26.54234	24.09725	1.7221266	1.437923
400	26.5297	23.09987	1.8740484	1.500008
500	26.51872	21.79603	2.104966	1.589739

Table 2. Information obtained from XRD examination of thin CdS films of different thicknesses.

thicknesses (nm)	2θ(deg)	(hkl) plans	d(Å) from Bragg's formula	d(Å) ICSD	a(Å) from XRD result	c(Å) from XRD result	a (Å) ICSD	c(Å) ICSD
200	26.56651	(0 0 2)	3.352551	3.3575	4.11356	6.705103	4.14	6.715
	24.901	(1 0 0)	3.572885	3.5853				
	28.352	(1 0 1)	3.145349	3.16275				
300	26.54234	(0 0 2)	3.355549	3.3575	4.117238	6.711099	4.14	6.715
	24.85	(1 0 0)	3.580102	3.5853				
	28.352	(1 0 1)	3.145349	3.16275				
	47.859	(1 0 3)	1.899104	1.8987				
400	26.5297	(0 0 2)	3.357119	3.3575	4.119165	6.714239	4.14	6.715
	24.914	(1 0 0)	3.57105	3.5853				
	28.226	(1 0 1)	3.159103	3.16275				
	47.751	(1 0 3)	1.903147	1.8987				
500	26.51872	(0 0 2)	3.358485	3.3575	4.12084	6.716969	4.14	6.715
	28.152	(1 0 1)	3.167238	3.16275				
	47.711	(1 0 3)	1.904649	1.8987				

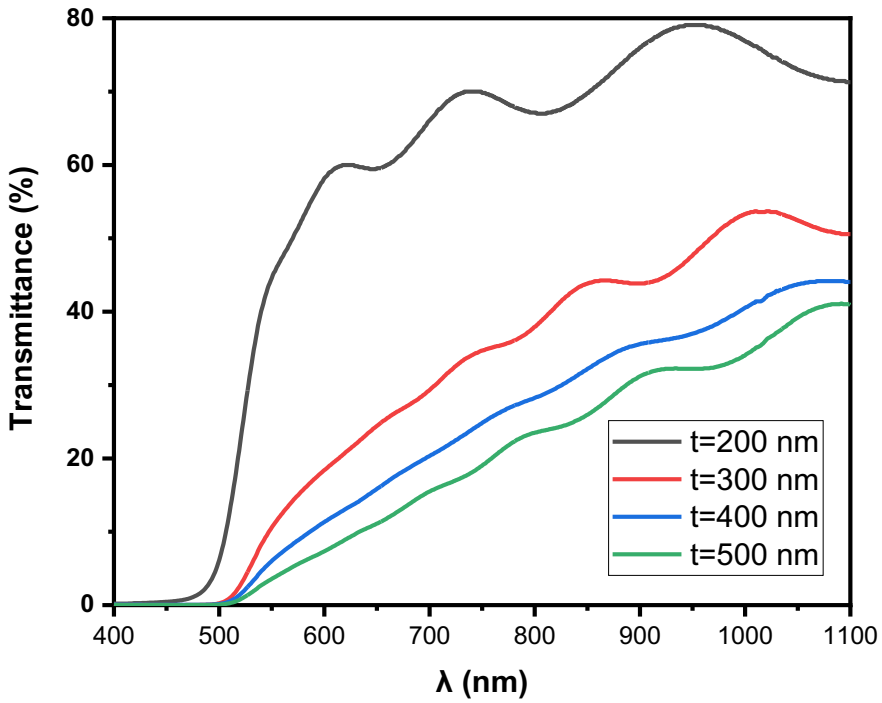

Fig. 3. thin CdS films grown at varying thicknesses with regard to optical transmission profiles.

(002) plane.

The following equation was used to determine the lattice parameters [20]:

$$\frac{1}{d^2} = \frac{4(h^2 + hk + k^2)}{3a^2} + \frac{l^2}{c^2} \quad (4)$$

where the inter-planer spacing is d (determined by Bragg's law), miller indices are (h k l), and the lattice constants are a and c. According to Table 2, the (002), (100), (101), and (103) plans reflect the d-spacing and the corresponding significant

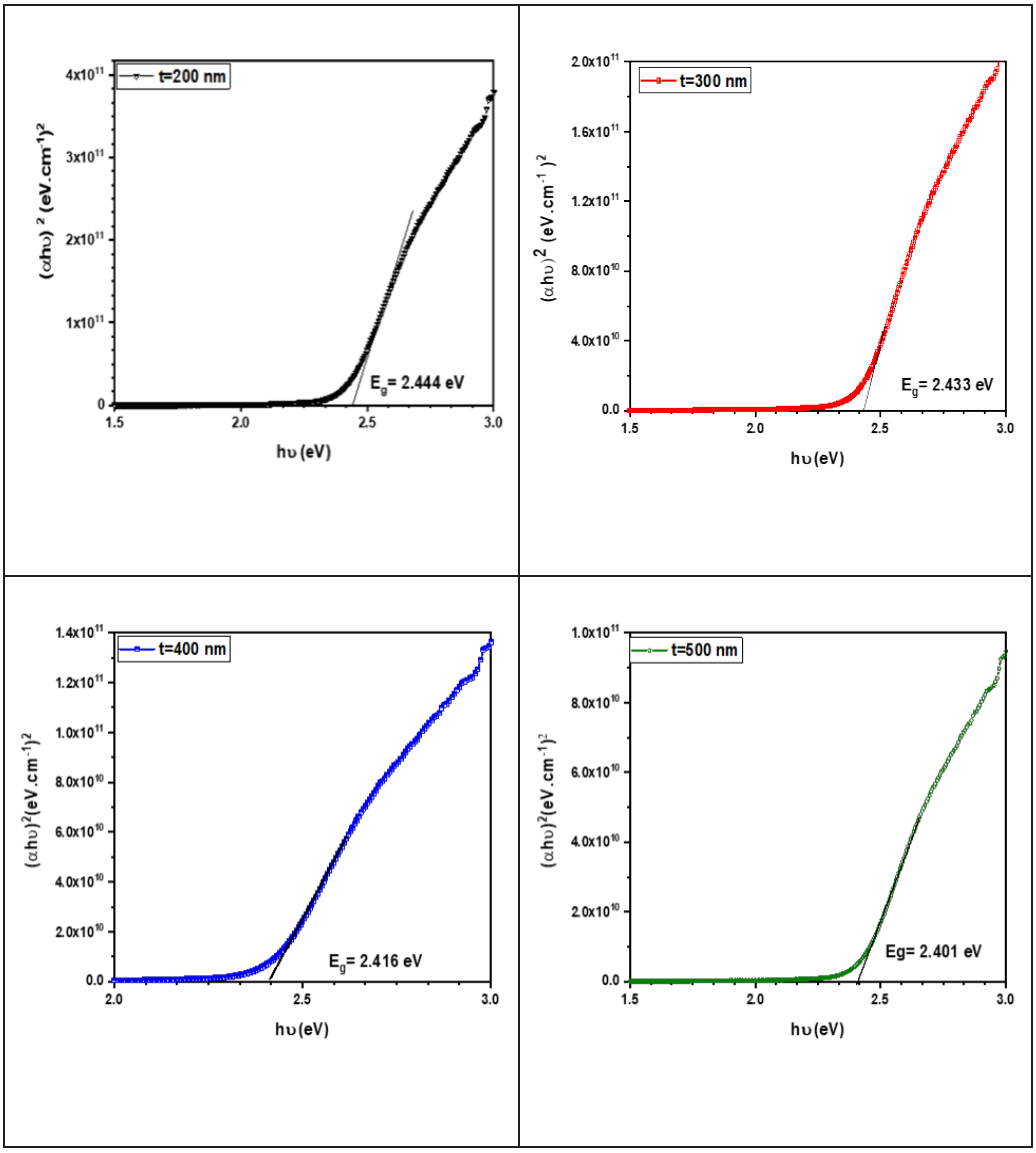

Fig. 4. Energy bandgap with varying thickness

peaks in a way that is consistent with the ICSD data. Table 2 shows that the increase in stress causes the lattice constants of the film at different thicknesses to be smaller than those of the bulk material.

Optical properties

More information regarding the optical characteristics of thin CdS films produced at room temperature and with different thicknesses is required. Investigations into transmission are conducted in the 200–1100 nm range. Transmittance in the visible range is quite low, increasing to just around 500 nm at longer wavelength areas where interference fringes are more obvious. As demonstrated in Fig. 3, films made at t = 200 nm appeared to have the highest crystallinity and the maximum transmission of any films made. The absorption edge has also moved to larger wavelength ranges, according to transmittance spectra, which has caused the optical band gap to narrow as the thickness of the material increases. Due to this feature, thin CdS films are advantageously used in heterostructure solar cells as absorbers.

According to the relationship, the band gap (Eg)

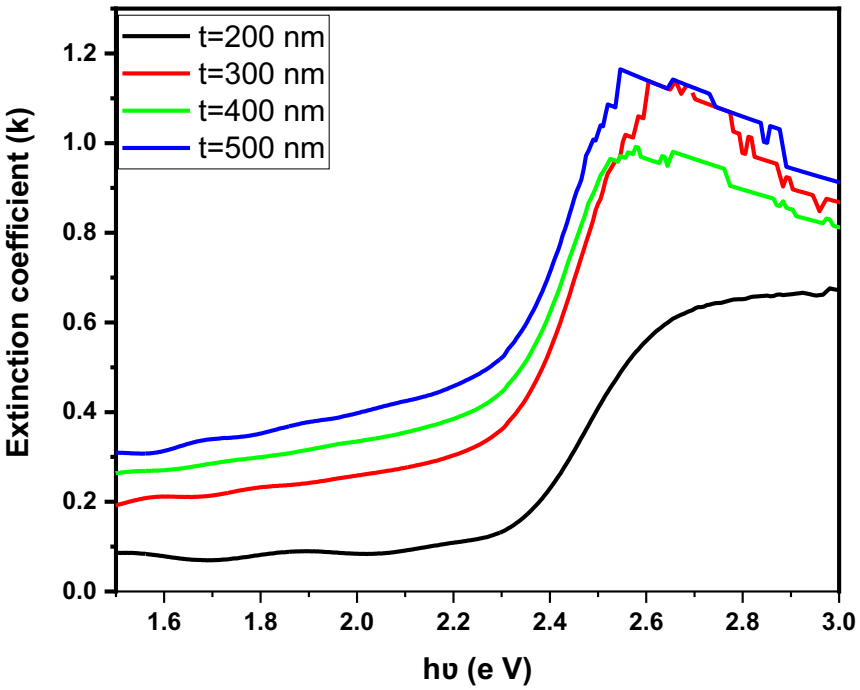

Fig. 5. Spectrum of CdS films of various thicknesses' extinction coefficients (k).

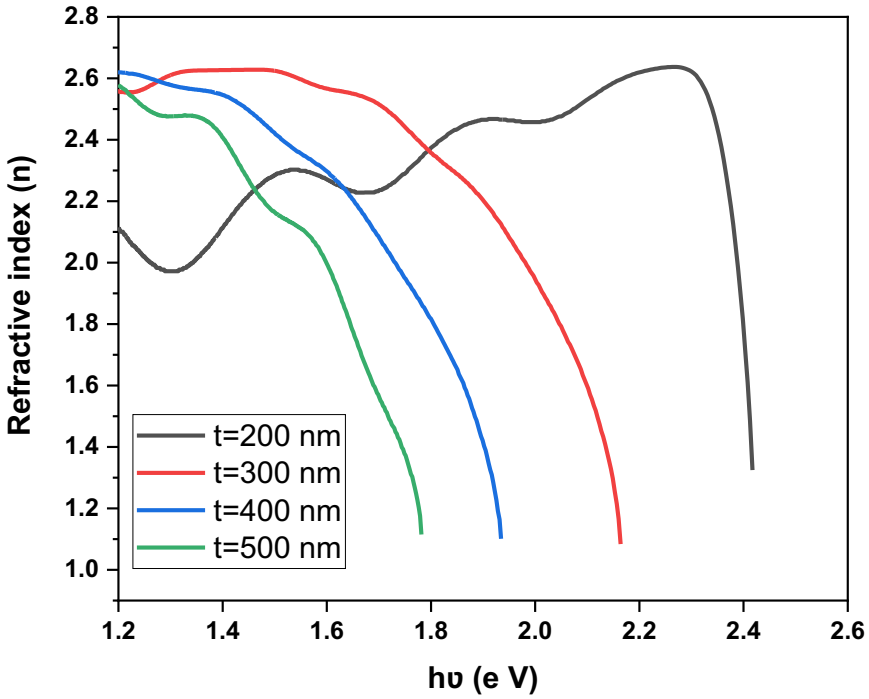

Fig. 6. With different thicknesses, the refractive index is spectrally dependent.

and absorption coefficient (α) are connected.

$$(\alpha h\upsilon)^2 = A(h\upsilon - E_g) \quad (5)$$

h is the plank's constant, and A is also a constant in this situation. Fig. 4 illustrates how to plot $(\alpha h\nu)^2$ versus hν using the Tauc plot and extend the line on the straight portion of the graph for absorption coefficients with zero values; there has been computation of the direct energy band gap. The linear dependency in the figure indicates that CdS is a semiconductor with a direct band gap. As the thickness increased, the band gap value started to fall between 2.444 and 2.401 eV; this drop in the band gap may be due to a decrease of nanoparticles.

The extinction coefficient (k), which offers important information on the substance's relationship to incoming light absorption, was calculated using a standard relation.

$$k = \frac{4\lambda}{4\pi} \quad (6)$$

Fig. 5 illustrates how variations in the extinction coefficient change with photon energy. Light absorption directly affects how much and how quickly the extinction coefficient changes. More light is absorbed at the grain boundaries in polycrystalline films. Thus, at photon energies below the basic absorption edge, k has a non-zero value.

The refractive index of a material, which is connected with its transmittance, local field, and ion polarizability in terms of electronic polarization, is one of its fundamental properties. Fig. 6 displays the distribution of n in relation to photon energy for films manufactured with various thicknesses. In general, the refractive index drops as film thickness rises, which can be a result of the films' decreasing crystallinity.

CONCLUSION

In CdS, various thicknesses of thin films have been produced. Findings from the X-ray diffraction investigation demonstrate that hexagonal CdS phases were prepared in every film, with typical grain sizes varying between 23.6 and 21.7 nm. Additionally, it was discovered that as film thickness increased, stress increased and dislocation per unit volume decreased for the deposited films. The spectrum dependences of optical transmittance provide information on where the fundamental absorption edge is located, and this placement matches the results characteristic of the compound CdS. With increasing film thickness, the film's refractive index fell and band gap values dropped from 2.444 to 2.401 eV. We can draw two conclusions: first, that the distinctive qualities of a film are significantly influenced by its thickness, and second, that the thermal evaporation method is very effective for creating CdS thin films.

CONFLICT OF INTEREST

The authors declare that there is no conflict of interests regarding the publication of this manuscript.

REFERENCES

1. Yılmaz, S., et al., Enhancement in the optical and electrical properties of CdS thin films through Ga and K co-doping. Materials Science in Semiconductor Processing, 2017. 60: p. 45-52.
2. Huang, L., et al., Electronic and optical properties of CdS films deposited by evaporation. Journal of Alloys and Compounds, 2015. 648: p. 591-594.
3. Shkir, M., et al., A facile spray pyrolysis fabrication of Sm:CdS thin films for high-performance photodetector applications. Sensors and Actuators A: Physical, 2020. 306.
4. Jassim, S.A.-J., A.A.R.A. Zumaila, and G.A.A. Al Waly, Influence of substrate temperature on the structural, optical and electrical properties of CdS thin films deposited by thermal evaporation. Results in Physics, 2013. 3: p. 173-178.
5. Kariper, A., et al., The structural, electrical and optical properties of CdS thin films as a function of pH. Materials Chemistry and Physics, 2011. 129(1-2): p. 183-188.
6. Petrus, R.Y., et al., Optical-Energy Properties of CdS Thin Films Obtained by the Method of High-Frequency Magnetron Sputtering. Optics and Spectroscopy, 2019. 126(3): p. 220-225.
7. Memarian, N., et al., Deposition of Nanostructured CdS Thin Films by Thermal Evaporation Method: Effect of Substrate Temperature. Materials (Basel), 2017. 10(7).
8. Mahmood, W., et al., Optical and electrical studies of CdS thin films with thickness variation. Optik, 2018. 158: p. 1558-1566.
9. Yücel, E. and O. Şahin, Effect of pH on the structural, optical and nanomechanical properties of CdS thin films grown by chemical bath deposition. Ceramics International, 2016. 42(5): p. 6399-6407.
10. Aboud, A.A., et al., The effect of Cu-doping on CdS thin films deposited by the spray pyrolysis technique. Journal of Materials Research and Technology, 2019. 8(2): p. 2021-2030.
11. Chander, S. and M.S. Dhaka, Optical and structural constants of CdS thin films grown by electron beam vacuum evaporation for solar cells. Thin Solid Films, 2017. 638: p. 179-188.
12. Shkir, M., et al., An investigation on structural, morphological, optical and third order nonlinear properties of facilely spray pyrolysis fabricated In:CdS thin films. Superlattices and Microstructures, 2019. 133.

13. Yılmaz, S., The investigation of spray pyrolysis grown CdS thin films doped with flourine atoms. Applied Surface Science, 2015. 357: p. 873-879.
14. Punitha, K., et al., Influence of post-deposition heat treatment on optical properties derived from UV–vis of cadmium telluride (CdTe) thin films deposited on amorphous substrate. Applied Surface Science, 2015. 344: p. 89-100.
15. Liu, B., et al., Effects of deposition temperature and CdCl2 annealing on the CdS thin films prepared by pulsed laser deposition. Journal of Alloys and Compounds, 2016. 654: p. 333-339.
16. Islam, M.A., et al., Comparison of Structural and Optical Properties of CdS Thin Films Grown by CSVT, CBD and Sputtering Techniques. Energy Procedia, 2013. 33: p. 203-213.
17. Chuu, D.S. and C.M. Dai, Quantum size effects in CdS thin films. Phys Rev B Condens Matter, 1992. 45(20): p. 11805-11810.
18. Noori, E.M. Effect of Gamma irradiation on the structural and optical properties of cadmium telluride thin films. in Journal of Physics: Conference Series. 2021. IOP Publishing.
19. Noori, E.M., Irradiation effect in cdse thin films. Journal of College of Education, 2019. 1(1).
20. Noori, E.M., Structure and optical properties of cdse thin films as a function of the annealing time. Al-Mustansiriyah Journal of Science, 2016. 27(5): p. 102-108.